Accepted manuscript

The Ameliorative and Neuroprotective Effects of Dietary Fiber on Hyperuricemia mice : A perspective from Microbiome and Metabolome

Yu Wang[1,2] Fengping Miao[1] Jun Wang[1,2] Maokun Zheng[4] Feng Yu[5] Yuetao Yi[1,3]*

[1]Yantai Institute of Coastal Zone Research, Chinese Academy of Sciences, Yantai, China. E-mail: ytyi@yic.ac.cn.

[2]University of Chinese Academy of Sciences, Beijing, China.

[3]Shandong Saline-Alkali Land Modern Agriculture Company, Dongying , China.

[4]Shandong First Medical University & Shandong Academy of Medical Sciences, Jinan,China.

[5]Department of Gastroenterology, Zibo Central Hospital, Zibo, Shandong, China.

*Corresponding author: E-mail: ytyi@yic.ac.cn.

Accepted manuscript

Abstract

The effect of single dietary fiber (DF) on lowering uric acid (UA) level has been reported in the literature. However, the potential protective mechanism of dietary fibre against potassium oxybate-induced hyperuricaemia (HUA), as modelled by prophylactic administration, remains unclear.The data demonstrates that DF significantly decreased serum and cerebral tissue UA concentrations, inhibited xanthine oxidase (XOD) expression and activity in the liver, and reduced levels of creatinine (Cr) and urea nitrogen (BUN) in the serum. Additionally, it mitigated the deposition of amyloid-β (Aβ) in cerebral tissue. Correlation analysis showed that DF modulated the TLR4/NF-κB signaling pathway, attenuating oxidative stress and inflammatory responses in HUA mice. Additionally, DF helps to maintain the composition of the gut microbiota, reducing harmful *Desulfovibrio* and enriching beneficial *Akkermansia* and *Ruminococcus* populations.The results of the faecal metabolomics analysis indicate that DF facilitates the regulation of metabolic pathways involved in oxidative stress and inflammation. These pathways include pyrimidine metabolism, tryptophan metabolism, nucleotide metabolism, and vitamin B6 metabolism. Additionally, the study found that DF has a preventive effect on anxiety-like behaviour induced by HUA. In summary, DF shows promise in mitigating HUA and cognitive deficits, primarily by modulating gut microbiota and metabolites.

Keywords: Hyperuricemia: Dietary fiber: Microbiome: Metabolome:Anxiety

Introduction

Hyperuricaemia (HUA) is a metabolic disease caused by a disorder of purine metabolism in the body, which further progresses to gout. According to the Global Burden of Disease (GBD) study, and the number of patients with HUA and gout is still likely to increase further in the coming years due to changes in modern dietary patterns, as well as gut microbiota dysbiosis [1; 2]. It has been found that patients with HUA have an imbalanced gut microbiota, characterised by reduced microbial diversity and significant changes in metabolic pathways and metabolites[3]. Similarly, gut microbes are important for body purine homeostasis and serum UA (SUA) levels [4; 5; 6]. The study shows that colonization of gnotobiotic mice with purine-degrading bacteria modulates levels of UA and other purines in the gut and systemically[7]. Asymptomatic patients with HUA have a higher abundance of short-chain fatty acid-producing bacteria than those with HUA [8; 9]. At the same time, abnormalities in the urea cycle may also trigger a variety of neurological problems such as Alzheimer's disease [10]. Several cross-sectional studies have shown that as blood UA levels rise, memory and executive abilities, among others, decline[11]. This suggests that there may be a strong link between UA levels and cognitive performance.

Dietary fibre (DF), a carbohydrate that cannot be digested by the body, has been extensively studied in the treatment of a variety of metabolic disorders[12]. In the absence of dietary fibre, the gut microbiota tends to produce mucus-degrading enzymes, resulting in thinning of the mucus layer, impairment of the barrier and increased intestinal permeability[13; 14]. Research has demonstrated that dietary fibres, such as inulin, β-polyglucan, and oligogalactose, either alone or in combination, have varying effects on the structure of gut microbiota[15]. Additionally, studies have found a significant negative correlation between total and grain fibre intake and UA levels in both Chinese and American adult populations[16; 17]. In contrast, inulin dietary fibre supplementation reduced UA levels in Uoxknockout mice by modulating gut microbes[18]. This demonstrates the regulatory effect of dietary fibre on gut microbiota and provides new ideas for therapeutic research and neuroprotection in hyperuricemia. Currently, the focus of dietary fibre intervention in hyperuricemia has been on therapeutic administration, with a concentration on immunomodulatory effects and gut microbial perspectives. However, the importance of diverse DF in humans as omnivores and the protective role of gut microbiota during the disease process have been neglected. It is important to consider these factors in future research.

Accepted manuscript

The aim of this study was to investigate the UA-lowering effects of single and complex dietary fibres, drugs, and probiotics in a mice model of Potassium oxyzinate (PO) induced HUA using a preventive dosing approach[19]. Additionally, the study examined the effects of these interventions on gut microbiology and metabolism. The study demonstrated that DF supplementation could be significant in preventing HUA and provides new evidence that dietary modification can effectively prevent the onset of chronic metabolic diseases[20].

2.Materials and methods

2.1 Materials and reagents

The Complex dietary fiber utilized in this study was a proprietary internal laboratory formulation (inulin 60%, polydextrose 15%, Xylo-oligosaccharide 10%, L-arabinose 8%, oligogalactose 5%, chitosan 2%), They were purchased from Shandong Balongchuangyuan Bio-technology Co..The inulin (Beneo™ HP-Gel) was obtained from Orafti (Oreye, Belgium) and polymerized 5-60.The probiotic supplement (Qingfeng probiotic solid beverage) was acquired from Huada Gene Co., Ltd., (Shenzhen, China), with specific details provided in Fig. S1. In addition, the similarity of the mechanism of action of probiotics, as common and effective supplements for regulating gut microbiota, could provide a comparison for the intervention effect of dietary fibre. Allopurinol (AP) was purchased from green leaf Biotechnology Co., Ltd. (Shanghai, China). Potassium oxonate (PO) were purchased from Sigma-Aldrich (St. Louis, MO, USA), which is a drug that induces a HUA model by inhibiting UA oxidase (UOX) activity[7]. Mouse IL-6, IL-1β, IL-10, TNF-α, XOD, GSH-PX, Aβ, TLR4, and NF-κB Elisa kits were obtained from Collaborative Pharmaceutical Bioengineering (Jiangsu, China). Mouse serum BUN, Cr, UA, MDA, and SOD kits were procured by Jiancheng Bioengineering Institute (Nanjing, China). Other chemical reagents used in this experiment were purchased from China National Pharmaceutical Group Chemical Reagent Co., Ltd.

2.2. Experimental design

Male KM mice (5 weeks old, 36-38g) were acquired from Jinan Pengyue Experimental Animal Breeding Center, Shandong, China, and housed at Binzhou Medical College Animal Experiment Center (Yantai, China). The mice were kept in a controlled environment (20-22°C) with a 12-hour light-dark cycle. All experiments adhered to the NIH Guidelines for Care and Use of Laboratory Animals (NIH Publication No. 8023, revised 1978) and were

approved by the Yantai Institute of Coastal Zone Research, Chinese Academy of Sciences (approval no.KJ-LL-005).

Following one-week acclimatization period, mice were randomly divided into 7 groups, with 7 animals in each group. Including a normal group (N, 0.5% CMC-Na + normal saline), a model group (M, 350 mg/kg PO in 0.5% CMC-Na + normal saline), a positive groups (AP, 350 mg/kg PO in 0.5% CMC-Na + 5 mg/kg AP), a probiotic supplement group (Pro-S, 350 mg/kg PO in 0.5% CMC-Na + 250 mg/kg Pro-S), a inulin dietary fiber group (IDF, 350 mg/kg PO in 0.5% CMC-Na + 4000 mg/kg IDF), a complex dietary fiber group (CDF, 350 mg/kg PO in 0.5% CMC-Na + 4000 mg/kg CDF), and a low-dose complex dietary fiber group (L-CDF, 350 mg/kg PO in 0.5% CMC-Na + 1500 mg/kg CDF). The dosage of intragastric administration was the equivalent dose converted by the surface area of the human. The treatment protocol is detailed in Fig.1A. Administration methods included intraperitoneal injection for model induction and intragastric administration for treatment, with a 6-hour interval between procedures. Mice were monitored and weighed weekly for three weeks. Behavioral analyses were conducted one day post-final administration. Post-euthanasia, gut tissues, feces, blood, and kidney tissues were collected for further analysis. Sample Collection: The mice were regularly fed and watered until the experiment conclusion. They were euthanized using pentobarbital anesthesia (50 mg/kg, intraperitoneal) at the experiment's end. Blood samples were allowed to stratify, followed by serum extraction via centrifugation at 4 °C, $1000\times$ g for 15 min, and stored at -80 °C for biochemical assays. The liver and cerebral tissues were harvested, weighed, and flash-frozen in liquid nitrogen, then stored at -80°C.

2.3 Determination of biochemical indicators

Serum UA (SUA), Cerebral UA (CUA), blood urea nitrogen (BUN), malondialdehyde (MDA), and creatinine (Cr) levels were measured using commercial kits from Nanjing Jiancheng Biotechnology, following the instructions. Levels of Toll-like receptor 4 (TLR4), nuclear factor kappa B (NF-κB), liver xanthine oxidase (XOD), superoxide dismutase (SOD), glutathione peroxidase (GSH-Px), and serum interleukins (IL-6, IL-1β, IL-10) and tumor necrosis factor-alpha (TNF-α) were quantified using ELISA kits from Nanjing Enzyme Immunoassay Biotechnology.

2.4 Behavioral testing

The Open-Field Test (OFT) evaluates the autonomous behavior, anxiety-like behavior, and stress of experimental animals in new environments. We used OFT to assess the neuroprotective effect of dietary fiber in mice. The apparatus consisted of a 50×50×35 cm black plastic box (width × length × height), with the bottom divided into 16 grids. The central four grids formed the central zone, while the surrounding 12 grids were designated as the peripheral zone. A mouse was placed in the center of the arena, and its movements were recorded for 10 minutes by a video camera. Behavioral data were analyzed using the VisuTrack animal behavior analysis system (Shanghai XinRuan Information Technology Co., Ltd, China). After each test, the box was cleaned with 75% alcohol to remove olfactory cues.

2.5 DNA extraction and sequence analysis of fecal samples

Fresh fecal samples from each mice were collected in individual sterile EP tubes at week 4, then immediately frozen in liquid nitrogen and stored at -80 °C. The bacterial genomic DNA was extracted from the fecal samples using an E.Z.N.A.® soil DNA Kit as per the manufacturer's instruction. The extracted genomic DNA was amplified with barcoded conventional primer pairs 338F (5'-ACTCCTACGGGAGGCAGCAG-3') and 806R (5'-GGACTACHVGGGTWTCTAAT-3') based on the bacterial 16S rRNA gene V3–V4 hypervariable region. The resulted PCR products were extracted from a 2% agarose gel, purified using an AxyPrep DNA Gel Extraction Kit (Axygen Biosciences, USA), and further quantified using the Quantus™ Fluorimeter (Promega, USA). The purified amplicons were pooled in equal amounts and paired-end sequenced (2 × 300 bp) on an Illumina MiSeq platform following the standard protocols at Shanghai Majorbio BioPharm Technology Co., Ltd. (Shanghai, China). The 16S rDNA sequencing raw data were deposited in NCBI Sequence Read Archive (SRA) under the accession number PRJNA1041986. OTU clustering and taxa annotation (taxa relative abundance analysis and genus evolutionary analysis), multi-sample comparative analysis (NMDS analysis and LEfSe analysis), the significance test of community structural differences among the groups (ANOSIM analysis) were used for sequence analysis. Taxa with significant differences among the groups were analyzed by MetaStat, and the correlations between microbiota and metabolites were analyzed by Spearman correlation analysis.

2.6 Non-targeted metabolomics analysis

The fecal samples was added to a centrifuge tube and a diameter grinding bead was added. 400 μL of extraction solution (methanol: water = 4:1 (v:v)) containing 0.02 mg/mL of internal standard (L-2-chlorophenylalanine) was used for metabolite extraction， and then centrifuged to remove the supernatant. The supernatant was collected after centrifugation, and the samples were analyzed The samples were gradient-eluted using a HSS T3 chromatographic column (100 × 2.1 mm, 1.8 μm, Waters, USA) with a flow rate of 0.40 mL/min and a column temperature of 40 °C. The Q Exactive™ HF-X mass spectrometer was operated in the positive and negative polarity modes. Then, the R package "ropls"(Version 1.6.2) was used to perform principal component analysis (PCA) and orthogonal least partial squares discriminant analysis (OPLS-DA). The metabolites with VIP>1, P<0.05 were determined as significantly different metabolites. through metabolic enrichment and pathway analysis based on KEGG database. Python packages "scipy.stats" was used to perform enrichment analysis to obtain the most relevant biological pathways for experimental treatments.

2.7. Statistical analysis

Statistical Analysis All bar graphs in this study were generated using GraphPadPrism 9.0, and the data are reported as the standard deviation of the means. Data were tested for normality and homogeneity of variance by SPSS 26.0 using the Shapiro-Wilk-test and F test, respectively. If the data satisfy normal distribution and, the student t test was used. If the data did not satisfy normality and chi-square, the Mann-Whitney-U test was used with significance set at P < 0.05. Some of the figures were created using BioRender (www.biorender.com).

3. Results

3.1. Effects of DF on SUA, Cr and BUN levels in HUA mice

In terms of body weight changes, Tn the M group had a significantly lower body weight gain than the N group, and the rest of the groups were not significantly different from the N group (Fig. 1B). Compared with the N group, the SUA level in the M group was significantly higher (P < 0.001), indicating that the HUA model induced by potassium oxonate was successful. In contrast, SUA levels were significantly lower in the AP, Pro-S, IDF, CDF, and L-CDF groups (Fig. 1C). We also observed that compared with the N group, the BUN and Cr levels in the M group were significantly higher (P < 0.001;P < 0.001). Whereas the serum

BUN and Cr levels of in the AP, IDF, CDF, and L-CDF groups were significantly lower (Fig. 1D,E). Therefore, we concluded that DF could effectively reduce UA levels, and achieved similar effects with AP and Pro-S groups, protecting the normal operation of renal function.

3.2. Effect of DF on XOD activity and content

Compared to the N group xanthine oxidase (XOD) activity and content in liver tissues were elevated by 68 % and 43 % in the model group (Fig. 2A and B). Meanwhile, liver XOD activity and content were significantly reduced after AP intervention compared to M group. Xanthine oxidase (XOD) activity was reduced by 28%, 25%, 26%, 24% and 13% in the liver tissues of AP, Pro-S, IDF, CDF, and L-CDF groups. However L-CDF failed to significantly reduce XOD activity in HUA mice. Respectively, compared to the M group. And in xanthine oxidase (XOD) content AP, Pro-S, IDF, CDF and L-CDF groups were reduced by 27%, 23%, 18%, 16% and 14%.

3.3. DF slows down oxidative stress and inflammatory responses

The study revealed that levels of SOD and GSH-Px were significantly lower in the liver tissue of the M group ($P < 0.001$ for both), as shown in Figure. 3C,D. In contrast, these levels were notably higher in the AP, Pro-S, IDF and CDF groups compared to the M group. Specifically, while the GSH-Px levels were significantly increased in the L-CDF group, no significant change was observed in SOD levels. Additionally, as a critical marker of oxidative damage, MDA levels were significantly elevated in the M group (Fig. 3E). However, these levels were substantially reduced in the AP, Pro-S, IDF and CDF groups. This suggests that both DF reduced oxidative damage induced by HUA.

TLR4/NF-κB pathway as an important pathway of inflammatory response, we did quantitative detection of TLR4 and NF-κB in mice cerebral tissue. Compared with the N group, the levels of TLR4 and NF-κB were significantly increased in the M group (Fig. 3A,B), while the levels of inflammatory factors IL-1β and IL-6 and TNF-α were significantly elevated in the serum (Fig. 3G-I). This indicated that potassium oxonate-induced mice were in an inflammatory state. In contrast, all these indicators were significantly reduced in the AP group. Under the intervention of dietary fibre, compared with the M group, the CDF group and L-CDF group significantly reduced the NF-κB content, and TLR4 also showed a decreasing trend, but there was no significant relationship. This result was similar to the Pro-S group. Compared with the N group, the serum levels of IL-6, IL-1β, and TNF-α were significantly increased and the anti-inflammatory factor IL-10 was significantly decreased in the M group (Fig. 3F). This suggests that, in the overall view, AP, Pro-S and DF can reduce the levels of IL-6, IL-1β, TNF-α and increase the level of IL-10 to different degrees.

However, it is worth noting that the L-CDF group did not show significant changes from the M group.

3.4. DF reduces Aβ deposition and alleviates neuroanxiety

Previous studies have shown that the urea cycle has an important role in normal cerebral cognitive function and that elevated UA may have an effect on behavioural cognition in mice[21; 22]. We did quantitative tests on UA and Aβ in cerebral tissue, and the results showed that the UA level was significantly increased in the cerebral of the M group compared with the N group(Fig. 4A). Compared with the M group, AP, Pro-S and IDF groups, CDF group L-CDF group were significantly decreased, which was consistent with the results of Serum UA assay. In addition, Aβ content was significantly deposited in the M group compared to the N group, and Aβ content was significantly reduced in the AP group, Pro-S group and IDF group, CDF group, and L-CDF group compared to the M group (Fig.4B). The results of the OFT showed 20 % reduction in the distance travelled compared to the N group in the M group (Fig. 4C). Compared to the M group Pro-S group and IDF group and CDF group were significantly higher. In addition, the HUA mice significantly reduced the exploration behaviour in the central region compared to the N group(Fig. 4D,E).The time of exploration in the central region was significantly higher in the AP, Pro-S and IDF and CDF groups than in the M group.

3.5 DF changed the structure of gut microbiota in HUA mice

3.5.1. Diversity analysis and species composition analysis of gut microbiota.

We investigated the relationship between gut microbiota changes and the development of hyperuricemia. Alpha diversity measures (Chao 1 and Shannon indices) and beta diversity were used to assess microbial diversity within and between groups. The results showed that interventions with AP, Pro-S, IDF, CDF and L-CDF significantly altered gut microbiota structure (Fig. 5A). Non-metric multidimensional scaling (NMDS) analysis revealed distinct differences in gut microbiota between M group and N group. The Pro-S and AP groups showed marked differences from the N group, indicating that allopurinol and probiotics, while reducing UA, significantly affected gut microbiota. In contrast, the IDF, CDF, L-CDF, and N groups showed minimal differences, suggesting that DF interventions could mitigate potassium oxonate's effects on mouce gut microbiota, maintaining a normal microbial composition (Fig. 5B). At the phylum level, dominant taxa included Firmicutes, Bacteroidetes, Actinobacteria, Proteobacteria, and Desulfobacteria. The M group, compared to the N group, showed an increased relative abundance of Desulfobacteria, which was suppressed in other intervention groups. In terms of Firmicutes/Bacteroidetes (F/B rate), the

F/B rate of HUA mice was higher than that of the N group, which was consistent with the results of Liu Xiu's study[23]. In contrast, in the AP group, there was a similar increasing trend in F/B, which may be related to the reduction of the relative abundance of Mycobacterium anomalum phylum by AP[24]. The F/B rate ratio, influenced by dietary interventions, mirrored that of the N group (Fig. S2). At the genus level, *Lactobacillus* abundance increased in the M, AP, and Pro-S groups, while groups receiving DF closely resembled the N group. These findings highlight DF supplementation's potential in preserving microbiota composition and structure in HUA mice (Fig. 5C).

3.5.2. Analysis of significant differences in the types of gut microbiota.

To assess the impact of AP, Pro-S, IDF, CDF and L-CDF on the mice gut microbiot with hyperuricemia, we conducted a comparative analysis to identify key differential biomarkers. In the M group, significant increases were observed in *Desulfovibrio, Streptococcus, norank_f_norank o_Clostridia_UCG-014,* and *norank f_Oscillospiraceae*, This is consistent with studies of diabetes and the gut-brain axis (Fig. 5D)[25; 26; 27; 28]. *Desulfovibrio*, known to impair the gut barrier and increase permeability, was notably abundant. AP enriched *Lactobacillus and norank f_norank o_Clostridia_UCG-014*, while reducing *Lachnospiraceae NK4A136 group*, *Rikenella*, *Mucispirillum*, and *Desulfovibrio* (Fig. S3). Pro-S resulted in an enrichment of *Lactobacillus* and *norank f_Eggerthellaceae*, and a decrease in *Rikenella*, *Mucispirillum*, and *Desulfovibrio* in the Pro-S group (Fig. S4). IDF increased the presence of GCA-900066575, *norank_f_Eubacterium_coprostanoligenes_group*, UCG-003 (Fig. S5). The L-CDF group saw an enrichment of *norank_f_norank_o_Clostridia_UCG-014*, *Akkermansia*, *norank_f_Ruminococcaceae*, *Parabacteroides*, and a decrease in *Candidatus_Saccharimonas*, *Anaerofustis* (Fig. S6). The CDF group experienced an increase in *Akkermansia*, *Muribaculum*, *Prevotellaceae_NK3B31_group*, and a reduction in *Lachnospiraceae_NK4A136_group*, *Desulfovibrio*, *Streptococcus* (Fig. 5E). These findings suggest that DF diminishes harmful bacterial colonization and promotes the growth of beneficial species such as *Akkermansia* and *Prevotellaceae*.

3.5.3. LEfSe analysis of gut microbiota.

To further explore microbial group alterations across the seven experimental groups, linear discriminant analysis effect size (LEfSe) analysis was performed. This method identified biomarkers and visualized dominant microorganisms through LDA score histograms and classification evolutionary branch diagrams (LDA > 4). LEfSe analysis revealed significant differences at the phylum level, particularly in Patescibacteria, Verrucomicrobiota, Desulfobacterota, Bacteroidota, and Firmicutes. At the genus level, notable differences were

found in *Akkermansia*, *Saccharimonas*, *Lachnospiraceae_NK4A136_group*, and *Desulfovibrio*, especially between the M group and the N group. After the supplementation of AP, *g_Lactobacillus* and other bacteria were enriched. After the supplementation of IDF, *g_Rikenella*, *f_Deferribacteraceae*, *g_Mucispirillum*, *p_Deferribacterota* and other bacteria were enriched. After the supplementation of CDF, *f_Muribaculaceae*, *f_Muribaculaceae*, *o_Bacteroidales*, *c_Bacteroidia* and other bacteria were enriched (Fig. S7).

3.6 Effect of CDF on metabolism of HUA mice

3.6.1. Metabolite spectrum analysis

PCA was utilized to detect outlier samples and cluster those with high similarity. The proximity of samples within the PCA plot reflects their similarity, with greater distances indicating more variability. The figure shows that the quality control (QC) samples are tightly clustered, demonstrating the LC-MS system's robust stability during the analytical process. A distinct separation trend was observed between the M group and the N group, AP group, IDF group, CDF group, and L-CDF group. Within each group, samples clustered cohesively, indicating significant metabolic variations between groups. The separation among the IDF, L-CDF, and CDF groups was less pronounced, consistent with expected results (Fig.6, A: cation, B: anion). Notably, the significant spatial distance between the dietary fiber intervention group and the M group highlights the effectiveness of DF intervention in regulating metabolic dysregulation of the gut microbiota caused by potassium oxonate.

3.6.2. Screening of differential metabolites

OPLS-DA revealed significant differences in fecal metabolites between the N group and the M group, as well as between the M group and the AP, Pro-S, IDF, CDF, and L-CDF groups. Differential metabolites were identified based on the variable importance in projection (VIP) score from the OPLS-DA model and Student's t-test P-value (VIP > 1, $P < 0.05$). A total of 1624 differential metabolites were identified through comparison and screening. Compared to the N group, levels of proline, tryptophan, tyrosine, 7-methylxanthine, and 7-deoxyguanosine significantly decreased in the M group ($P < 0.05$), while 7-methyladenine, arachidonic acid glycerol, myristic acid, 3,4,5,6-tetrahydrohippUA, N'-formylkynurenine, 5-hydroxyindoleacetic acid salt, and urochole significantly increased ($P < 0.001$). Conversely, compared to the M group, deoxyguanosine, adenine, oxypurine alcohol, 7-methyladenine, 1-methylguanine, hypoxanthine, and dihydrouracil were notably decreased in the H-CDF and IDF groups. Lysine, 7-methyladenine, deoxycholic acid, N-eicosapentaenyl tryptophan, and isoleucine were significantly reduced in the Pro-S group (Fig. 6C).

3.6.3. Analysis of differential metabolic pathways.

We utilized the scipy pathway analysis module to examine the metabolic functions of identified differential metabolites. The accompanying figure displays the top 20 pathways, encompassing protein digestion and absorption, arginine and proline metabolism, biosynthesis of phenylalanine, tyrosine, and tryptophan, ABC transporters, and nucleotide metabolism. Additionally, KEGG topological analysis was conducted to explore the differential metabolite pathways between groups ($P < 0.05$), specifically focusing on the top five pathways. This analysis unveiled significant differences in metabolic pathways influenced by complex dietary fiber to those affected by allopurinol and probiotic supplements. Notably, both the IDF group and the CDF group shared pathways in nucleotide and pyrimidine metabolism. Furthermore, the metabolic pathways involving alanine, aspartic acid, and glutamic acid were notably enriched in the AP group, CDF group, and L-CDF group, suggesting a positive effect on UA metabolism (Fig. 6D-I).

3.7. Correlation analysis of gut microbiota and metabolites.

Spearman correlation analysis identified a strong positive correlation between the genera such as *Lachnospiraceae NK4A136 group*, *Desulfovibrio*, and *Erysipelotrichaceae*, and various metabolites including hypoxanthine, urocholin hydrochloride, hydroxypurine, 2,6-dihydroxypurine, 2'-deoxyinosine, 3'-deoxyinosine, 4-methyl-2-oxopentanoic acid, and arachidonic acid ester. Conversely, these metabolites showed a negative correlation with *norank_f_Muribaculaceae*, *Prevotellaceae UCG-001*, *Ruminococcaceae*, *Akkermansia*, and *Prevotellaceae NK3B31 group*. Significantly, the *Prevotellaceae NK3B31 group* was positively correlated with short-chain fatty acids (SCFA) such as hydroxybutyric acid, and energy metabolism-related complexs including sucrose and succinic acid, as well as the antioxidant cysteine (Fig. 7).

3.8. Correlation analysis of gut microbiota and inflammatory factors

The images are Heatmap analyses of the correlation between UA, inflammatory factors (IL-1β, IL-6 and TNF-α), anti-inflammatory factors (IL-10) and gut microorganisms (genus level, abundance ranked in the top 20), respectively (Fig. 8). *norank_f_Erysipelotrichaceae*, *norank_f_norank_o_RF39*, *Desulfovibrio* and *Lachnospiraceae_NK4A136_group* were significantly positively correlated with UA levels, inflammatory factors, and significantly negatively correlated with anti-inflammatory factors ($P < 0.05$). Among them, *norank_f_Erysipelotrichaceae* was particularly significant in this relationship, which was similar to the results of previous studies[29]. *Alloprevotella*, *norank_f_norank_Clostridia_UCG-014 was* negatively correlated with UA levels, pro-inflammatory factors, and positively correlated with anti-inflammatory factors, which is

consistent with the results of previous studies on beneficial body effects[30]. Interestingly, *Enterorhabdus* showed a positive correlation with UA levels and inflammatory factors and a negative correlation with anti-inflammatory factors, which is consistent with the findings of Zhihong Zhang's team[31]. Rikenella showed a significant correlation with UA levels (P < 0.05), while similar results were found in a study of a mouse model of chronic renal failure induced using a 0.2% adenine diet[32].

4. Discussions

In this study, we compared the changes in gut microbiota and metabolites in HUA mice by three common interventions: drugs, probiotics, and dietary fibre (IDF and CDF) through the microbiome and metabolome. Previous studies have shown that single dietary fibre is an effective approach for the prevention and treatment of metabolic system disorders[33; 34]. It is worth noting that various dietary fibers contribute to the complex functions and interactions of gut microbiota. However, the combined effects of multiple dietary fibers on the prevention of HUA have not been thoroughly explored.

Studies have demonstrated that human UA is synthesized in the liver through urea catalysis by xanthine oxidase, and subsequently excreted through gut microbiota and renal filtration[35]. The excessive accumulation of UA can impair renal filtration and eventually lead to the development of gout[36]. Our finding indicate that DF has the ability to inhibit the activity and expression of XOD, thereby reducing UA production in the body. Additionally, based on the results of BUN and Cr, DF was found to protect normal kidney function in HUA mice by ensuring UA excretion and reducing its accumulation in vivo[37]. Furthermore, DF has been shown to up-regulate levels of SOD and GSH-Px while decreasing MDA production - an oxidative stress product. This serves to scavenge free radicals post-oxidative stress, improve antioxidant capacity, and reduce damage caused by oxidative stress within the body[38]. Oxidative stress damage coupled with fluctuations in gut microbiota can induce inflammatory factor production[39; 40]. The results demonstrate significant changes in pro-inflammatory and anti-inflammatory factors between the M group compared with the N group, indicating that HUA mice were experiencing an inflammatory state. This inflammatory response may be attributed to elevated UA levels, imbalanced i gut microbiota, as well as increased gut permeability among mice[41]. However, intervention with DF significantly altered this phenomenon - suggesting that supplementation with CDF can help reduce both production and accumulation of UA while also decreasing overall inflammatory responses within the

body. Moreover it helps protect normal kidney function.

In this study, we observed a significant shift in the composition of gut microbiota in HUA mice, particularly in the F/B ratio, which plays a crucial role in gut homeostasis and is implicated in hyperuricemia. Although the F/B ratio in the M group exceeded that of the N group, the difference was not statistically significant, consistent with findings from another preclinical study[42]. However, it is noteworthy that the drug and probiotic treatments notably deviated from this pattern. This emphasizes the necessity for further research to elucidate the relationship between the F/B ratio and hyperuricemia. Notably, under dietary fiber intervention, the F/B ratio approached normal levels, suggesting that while both drug and probiotic treatments reduced UA levels, they significantly altered gut microbiota. NMDS analysis supported these findings. At the phylum level, an increase in *Desulfobacter* and *Lachnospiraceae_NK4A136 group* was documented in the model group, consistent with previous studies[43]. *Desulfovibrio* is a detrimental bacterium found in human colonic microbiota; its presence can decrease goblet cell numbers and mucin production leading to compromised mucus barrier and increased gut permeability. This may facilitate lipopolysaccharide translocation into bloodstream triggering inflammation[44; 45]. Moreover, abundance of *Desulfovibrio* correlates with severity of neurological conditions such as Parkinson's disease[46; 47]. CDF intervention not only reduced *Lachnospiraceae_NK4A136* and *Desulfovibrio* populations but also enhanced beneficial acetic acid-producing bacteria like *AKK*, *Streptococcus*, and *UCG003*, as well as *Rhodospirillales*, which are conducive to gut barrier integrity that a benefit not mirrored in the drug treatment group. Given that HUA has been linked to Alzheimer's disease progression, our findings of reduced anxiety and improved exploratory behavior in HUA mice due to DF intake are significant[22; 48]. These behavioral changes, coupled with decreased UA,TLR4, NK-κB, and Aβ levels in the brain, parallel the benefits seen with IDF[49; 50], hinting at the potential of adequate DF consumption in preventing neurodegenerative disorders such as autism and Alzheimer's disease[51; 52; 53].

The accumulation of UA may precipitate renal acid-base imbalance, mitochondrial dysfunction, and acute kidney injury, while also enhancing renal glutamine and glutamate uptake[54; 55]. Elevated Aβ levels further influence NMDA receptor-mediated glutamine transformation, suggesting a potential glutamine and glutamate deficiency or overdrive in HUA mice[56; 57]. This study's KEGG pathway analysis revealed metabolic disturbances in tryptophan, citrate, and tyrosine metabolism within the model group, aligning with prior

research. Notably, CDF influenced various metabolic pathways akin to the AP group, with alanine, aspartate, glutamate metabolism, and pyrimidine metabolism potentially crucial in HUA prevention. Earlier studies have corroborated that glycine and tryptophan supplementation markedly lowers SUA in mild HUA[43; 58], highlighting their significant role in the citric acid cycle and tryptophan metabolism. Additionally, our findings suggest a distinct vitamin B6 metabolism under CDF supplementation. While vitamin B6 direct link to UA levels is not established, its association with cardiovascular, metabolic, and neurological diseases is well-recognized[59; 60], including its use in alleviating dexamethasone-induced depression[61; 62; 63]. Thus, the contributory role of vitamin B6 metabolism in UA reduction warrants further investigation. This study showed that although the Pro-S group , AP group and the DF intervention group were all effective in preventing the occurrence of HUA, it is worth noting that the DF group was different from the other two groups in that it was derived from food and could be obtained naturally, rather than chemically synthesized or cultured in vitro. In this perspective, DF interventions may be superior to traditional pharmacological and probiotic interventions in the disease prevention phase. This also suggests the importance of a balanced nutrient intake.

5. Conclusions

In summary, this study showed that DF inhibits UA production by regulating the structure and metabolism of gut microbiota, inhibiting hepatic XOD activity and reducing hepatic XOD expression, and also has anti-inflammatory, hepatoprotective, and anti-kidney injury effects, alleviating neurological damage in HUA mice. Compared with drug and probiotic group, it is more advantageous in maintaining the structure of gut microbiota. However, whether the positive therapeutic effects of CDF are mediated by changes in the gut microbiota should be further explored by faecal microbiota transplantation and targeting the metabolome. Our findings provide evidence that dietary fibre-gut microbiota interactions can alleviate HUA, as well as provide an important basis for the prevention and treatment of hyperuricemia through dietary modification[34; 64].

6. Acknowledgments

7. Author Contributions

Yu Wang: methodology, data analysis, software, visualisation and writing-original draft. Fengping Miao: conceptualization, resources,supervision, writing-original draft, and project administration. Yuetao Yi: conceptualization, data interpretation, supervision, funding acquisition, project administration, and writing-review & editing. Jun Wang: conceptualization and methodology. Maokun Zheng: resources and project administration. Feng Yu: conceptualization and resources.

8. Conflicts of interest

The authors declared no competing interests.

9. References

1. Rai SK, Fung TT, Lu N *et al.* (2017) The Dietary Approaches to Stop Hypertension (DASH) diet, Western diet, and risk of gout in men: prospective cohort study. *BMJ* **357**, j1794.

2. Kyu HH, Abate D, Abate KH *et al.* (2018) Global, regional, and national disability-adjusted life-years (DALYs) for 359 diseases and injuries and healthy life expectancy (HALE) for 195 countries and territories, 1990-2017: a systematic analysis for the Global Burden of Disease Study 2017. *The Lancet* **392**, 1859-1922.

3. Rakoff-Nahoum S, Foster KR, Comstock LE (2016) The evolution of cooperation within the gut microbiota. *Nature* **533**, 255-259.

4. Lv Q, Xu D, Zhang X *et al.* (2020) Association of Hyperuricemia With Immune Disorders and Intestinal Barrier Dysfunction. *Front Physiol* **11**, 524236.

5. Yin H, Liu N, Chen J (2022) The Role of the Intestine in the Development of Hyperuricemia. *Front Immunol* **13**, 845684.

6. Zhao F, Zhao Z, Man D *et al.* (2023) Changes in gut microbiota structure and function in gout patients. *Food Bioscience* **54**, 102912.

7. Tang DH, Ye YS, Wang CY *et al.* (2017) Potassium oxonate induces acute hyperuricemia in the tree shrew (tupaia belangeri chinensis). *Exp Anim* **66**, 209-216.

8. Martínez-Nava GA, Méndez-Salazar EO, Vázquez-Mellado J *et al.* (2023) The impact of short-chain fatty acid–producing bacteria of the gut microbiota in hyperuricemia and gout diagnosis. *Clinical Rheumatology* **42**, 203-214.

9. Dang K, Zhang N, Gao H *et al.* (2023) Influence of intestinal microecology in the development of gout or hyperuricemia and the potential therapeutic targets. *Int J Rheum Dis* **26**, 1911-1922.

10. Ju YH, Bhalla M, Hyeon SJ *et al.* (2022) Astrocytic urea cycle detoxifies Aβ-derived ammonia while impairing memory in Alzheimer's disease. *Cell Metab* **34**, 1104-1120.e1108.

11. Khaled Y, Abdelhamid AA, Al-Mazroey H *et al.* (2023) Higher serum uric acid is associated with poorer cognitive performance in healthy middle-aged people: a cross-sectional study. *Intern Emerg Med* **18**, 1701-1709.

12. Li L, Yan S, Liu S *et al.* (2023) In-depth insight into correlations between gut microbiota and dietary fiber elucidates a dietary causal relationship with host health. *Food Res Int* **172**, 113133.

13. Zarrinpar A, Chaix A, Yooseph S *et al.* (2014) Diet and feeding pattern affect the diurnal dynamics of the gut microbiome. *Cell Metab* **20**, 1006-1017.

14. Fu J, Zheng Y, Gao Y *et al.* (2022) Dietary Fiber Intake and Gut Microbiota in Human Health. *Microorganisms* **10**.

15. Tawfick MM, Xie H, Zhao C *et al.* (2022) Inulin fructans in diet: Role in gut homeostasis, immunity, health outcomes and potential therapeutics. *Int J Biol Macromol* **208**, 948-961.

16. Zhu Q, Yu L, Li Y *et al.* (2022) Association between Dietary Fiber Intake and Hyperuricemia among Chinese Adults: Analysis of the China Adult Chronic Disease and Nutrition Surveillance (2015). *Nutrients* **14**.

17. Sun Y, Sun J, Zhang P *et al.* (2019) Association of dietary fiber intake with hyperuricemia in U.S. adults. *Food Funct* **10**, 4932-4940.

18. Guo Y, Yu Y, Li H *et al.* (2021) Inulin supplementation ameliorates hyperuricemia and modulates gut microbiota in Uox-knockout mice. In *Eur J Nutr*, 2020/10/27 ed., vol. 60, pp. 2217-2230.

19. Khazaie S, Jafari M, Heydari J *et al.* (2019) Modulatory effects of vitamin C on biochemical and oxidative changes induced by acute exposure to diazinon in rat various tissues: Prophylactic and therapeutic roles. *J Anim Physiol Anim Nutr (Berl)* **103**, 1619-1628.

20. Takashi K (2021) Modification of Dietary Habits for Prevention of Gout in Japanese People: Gout and Macronutrient Intake. *American Journal of Health Research* **9**, 128-142.

21. Handley RR, Reid SJ, Brauning R *et al.* (2017) Brain urea increase is an early Huntington's disease pathogenic event observed in a prodromal transgenic sheep model and HD cases. *Proc Natl Acad Sci USA* **114**, E11293-e11302.

22. Mijailovic NR, Vesic K, Borovcanin MM (2022) The Influence of Serum uric acid on the Brain and Cognitive Dysfunction. *Front Psychiatry* **13**, 828476.

23. Liu X, Lv Q, Ren H *et al.* (2020) The altered gut microbiota of high-purine-induced hyperuricemia rats and its correlation with hyperuricemia. *PeerJ* **8**, e8664.

24. Sun Y, Xu D, Zhang G *et al.* (2024) Wild-type Escherichia coli Nissle 1917 improves hyperuricemia by anaerobically degrading uric acid and maintaining gut microbiota profile of mice. *Journal of Functional Foods* **112**, 105935.

25. Wang H, Shen Q, Fu Y *et al.* (2023) Effects on Diabetic Mice of Consuming Lipid Extracted from Foxtail Millet (Setaria italica): Gut Microbiota Analysis and Serum Metabolomics. *J Agric Food Chem* **71**, 10075-10086.

26. Yuan L, Zhao J, Liu Y *et al.* (2024) Multiomics analysis revealed the mechanism of the anti-diabetic effect of Salecan. *Carbohydr Polym* **327**, 121694.

27. Wu Y, Wang Y, Hu A *et al.* (2022) Lactobacillus plantarum-derived postbiotics prevent Salmonella-induced neurological dysfunctions by modulating gut-brain axis in mice. *Front Nutr* **9**, 946096.

28. Yan S, Chen J, Zhu L *et al.* (2022) Oryzanol Attenuates High Fat and Cholesterol Diet-Induced Hyperlipidemia by Regulating the Gut Microbiome and Amino Acid Metabolism. *J Agric Food Chem* **70**, 6429-6443.

29. Kaakoush NO (2015) Insights into the Role of Erysipelotrichaceae in the Human Host. *Front Cell Infect Microbiol* **5**, 84.

30. Downes J, Dewhirst FE, Tanner ACR *et al.* (2013) Description of Alloprevotella rava gen. nov., sp. nov., isolated from the human oral cavity, and reclassification of Prevotella tannerae Moore et al. 1994 as Alloprevotella tannerae gen. nov., comb. nov. *Int J Syst Evol Microbiol* **63**, 1214-1218.

31. Meng Y, Hu Y, Wei M *et al.* (2023) Amelioration of hyperuricemia by Lactobacillus acidophilus F02 with uric acid -lowering ability via modulation of NLRP3 inflammasome and gut microbiota homeostasis. *Journal of Functional Foods* **111**, 105903.

32. Wang R, Hu B, Ye C *et al.* (2022) Stewed Rhubarb Decoction Ameliorates Adenine-Induced Chronic Renal Failure in Mice by Regulating Gut Microbiota Dysbiosis. *Front Pharmacol* **13**, 842720.

33. Pan L, Han P, Ma S *et al.* (2020) Abnormal metabolism of gut microbiota reveals the possible molecular mechanism of nephropathy induced by hyperuricemia. *Acta Pharm Sin B* **10**, 249-261.

34. Zhang Y, Chen S, Yuan M *et al.* (2022) Gout and Diet: A Comprehensive Review of Mechanisms and Management. *Nutrients* **14**.

35. Srivastava A, Kaze AD, McMullan CJ *et al.* (2018) uric acid and the Risks of Kidney Failure and Death in Individuals With CKD. *Am J Kidney Dis* **71**, 362-370.

36. Chilappa CS, Aronow WS, Shapiro D *et al.* (2010) Gout and hyperuricemia. *Compr Ther* **36**, 3-13.

37. Leblanc M, Garred LJ, Cardinal J *et al.* (1998) Catabolism in critical illness: estimation from urea nitrogen appearance and creatinine production during continuous renal replacement therapy. *Am J Kidney Dis* **32**, 444-453.

38. Chaudhary P, Janmeda P, Docea AO *et al.* (2023) Oxidative stress, free radicals and antioxidants: potential crosstalk in the pathophysiology of human diseases. *Front Chem* **11**, 1158198.

39. Li Q, Lin L, Zhang C *et al.* (2024) The progression of inorganic nanoparticles and natural products for inflammatory bowel disease. *J Nanobiotechnology* **22**, 17.

40. Tomasello G, Mazzola M, Leone A *et al.* (2016) Nutrition, oxidative stress and intestinal dysbiosis: Influence of diet on gut microbiota in inflammatory bowel diseases. *Biomed Pap Med Fac Univ Palacky Olomouc Czech Repub* **160**, 461-466.

41. Bian M, Wang J, Wang Y *et al.* (2020) Chicory ameliorates hyperuricemia via modulating gut microbiota and alleviating LPS/TLR4 axis in quail. *Biomed Pharmacother* **131**, 110719.

42. Li X, Chen Y, Gao X *et al.* (2021) Antihyperuricemic Effect of Green Alga Ulva lactuca Ulvan through Regulating Urate Transporters. *J Agric Food Chem* **69**, 11225-11235.

43. Oshima S, Shiiya S, Nakamura Y (2019) Serum uric acid -Lowering Effects of Combined Glycine and Tryptophan Treatments in Subjects with Mild Hyperuricemia: A Randomized, Double-Blind, Placebo-Controlled, Crossover Study. *Nutrients* **11**.

44. Zhang K, Qin X, Qiu J *et al.* (2023) Desulfovibrio desulfuricans aggravates atherosclerosis by enhancing intestinal permeability and endothelial TLR4/NF-κB pathway in Apoe (-/-) mice. *Genes Dis* **10**, 239-253.

45. Fang J, Wang H, Zhou Y *et al.* (2021) Slimy partners: the mucus barrier and gut microbiome in ulcerative colitis. *Exp Mol Med* **53**, 772-787.

46. Murros KE, Huynh VA, Takala TM *et al.* (2021) Desulfovibrio Bacteria Are Associated With Parkinson's Disease. *Front Cell Infect Microbiol* **11**, 652617.

47. Huynh VA, Takala TM, Murros KE *et al.* (2023) Desulfovibrio bacteria enhance alpha-synuclein aggregation in a Caenorhabditis elegans model of Parkinson's disease. *Front Cell Infect Microbiol* **13**, 1181315.

48. Li LL, Ma YH, Bi YL *et al.* (2021) Serum uric acid May Aggravate Alzheimer's Disease Risk by Affecting Amyloidosis in Cognitively Intact Older Adults: The CABLE Study. *J Alzheimers Dis* **81**, 389-401.

49. Xu Y, Yang Y, Li B *et al.* (2022) Dietary methionine restriction improves gut microbiota composition and prevents cognitive impairment in D-galactose-induced aging mice. *Food Funct* **13**, 12896-12914.

50. Sun Y, Koyama Y, Shimada S (2022) Inflammation From Peripheral Organs to the Brain: How Does Systemic Inflammation Cause Neuroinflammation? *Front Aging Neurosci* **14**, 903455.

51. Nettleton JE, Klancic T, Schick A *et al.* (2021) Prebiotic, Probiotic, and Synbiotic Consumption Alter Behavioral Variables and Intestinal Permeability and Microbiota in BTBR Mice. *Microorganisms* **9**.

52. Hsiao EY, McBride SW, Hsien S *et al.* (2013) Microbiota modulate behavioral and physiological abnormalities associated with neurodevelopmental disorders. *Cell* **155**, 1451-1463.

53. Inoue R, Sakaue Y, Kawada Y *et al.* (2019) Dietary supplementation with partially hydrolyzed guar gum helps improve constipation and gut dysbiosis symptoms and behavioral irritability in children with autism spectrum disorder. *J Clin Biochem Nutr* **64**, 217-223.

54. Valdivielso JM, Eritja À, Caus M *et al.* (2020) Glutamate-Gated NMDA Receptors: Insights into the Function and Signaling in the Kidney. *Biomolecules* **10**.

55. Wang R, Halimulati M, Huang X *et al.* (2023) Sulforaphane-driven reprogramming of gut microbiome and metabolome ameliorates the progression of hyperuricemia. *J Adv Res* **52**, 19-28.

56. Olajide OJ, Chapman CA (2021) Amyloid-β (1-42) peptide induces rapid NMDA receptor-dependent alterations at glutamatergic synapses in the entorhinal cortex. *Neurobiol Aging* **105**, 296-309.

57. Wu GM, Du CP, Xu Y (2023) Oligomeric Aβ25-35 induces the tyrosine phosphorylation of PSD-95 by SrcPTKs in rat hippocampal CA1 subfield. *Int J Neurosci* **133**, 888-895.

58. Oshima S, Shiiya S, Nakamura Y (2019) Combined Supplementation with Glycine and Tryptophan Reduces Purine-Induced Serum uric acid Elevation by Accelerating Urinary uric acid Excretion: A Randomized, Single-Blind, Placebo-Controlled, Crossover Study. *Nutrients* **11**.

59. Han EH, Lim MK, Lee SH *et al.* (2018) Synergic effect in the reduction of serum uric acid level between ethanol extract of Aster glehni and vitamin B(6). *Food Sci Biotechnol* **27**, 1439-1444.

60. Zhang Y, Qiu H (2018) Folate, Vitamin B6 and Vitamin B12 Intake in Relation to Hyperuricemia. *J Clin Med* **7**.

61. Wang L, Li X, Montazeri A *et al.* (2023) Phenome-wide association study of genetically predicted B vitamins and homocysteine biomarkers with multiple health and disease outcomes: analysis of the UK Biobank. *Am J Clin Nutr* **117**, 564-575.

62. Mesripour A, Alhimma F, Hajhashemi V (2019) The effect of vitamin B6 on dexamethasone-induced depression in mice model of despair. *Nutr Neurosci* **22**, 744-749.

63. Theofylaktopoulou D, Ulvik A, Midttun Ø *et al.* (2014) Vitamins B2 and B6 as determinants of kynurenines and related markers of interferon-γ-mediated immune activation in the community-based Hordaland Health Study. *Br J Nutr* **112**, 1065-1072.

64. Wang J, Chen Y, Zhong H *et al.* (2022) The gut microbiota as a target to control hyperuricemia pathogenesis: Potential mechanisms and therapeutic strategies. *Crit Rev Food Sci Nutr* **62**, 3979-3989.
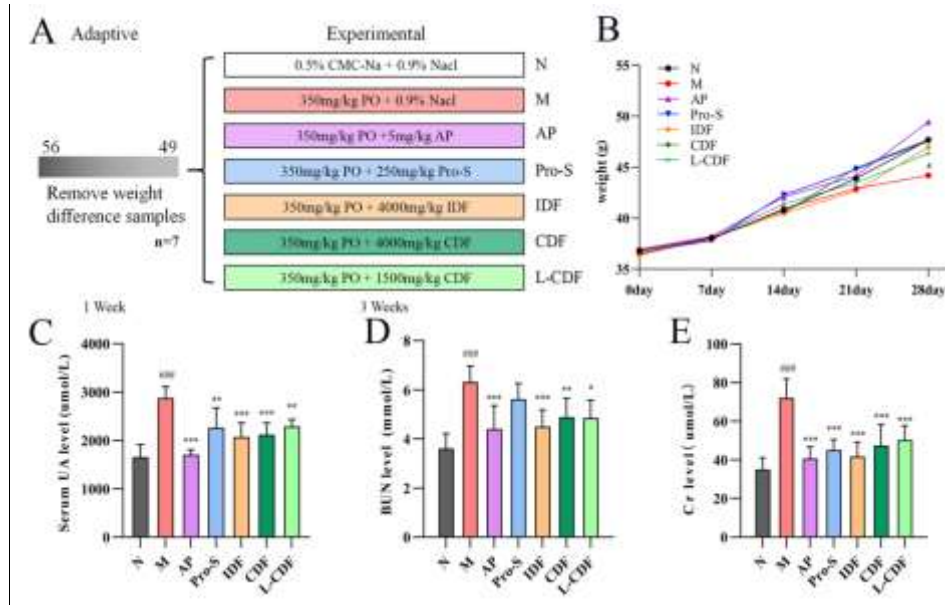
Fig. 1 DF reduced UA in HUA mice and its protective effect on kidney. A Experimental procedure. B Body weight changes. C Serum UA levels. D Serum urea nitrogen levels. E Serum creatinine levels. Data are presented as mean ± SD (n = 7 per group). *$P < 0.05$;**$P < 0.01$; ***$P < 0.001$ represent significance between each group compared with M group. #$P < 0.05$; ##$P < 0.01$; ###$P < 0.001$ represent significance between M group compared with N group.
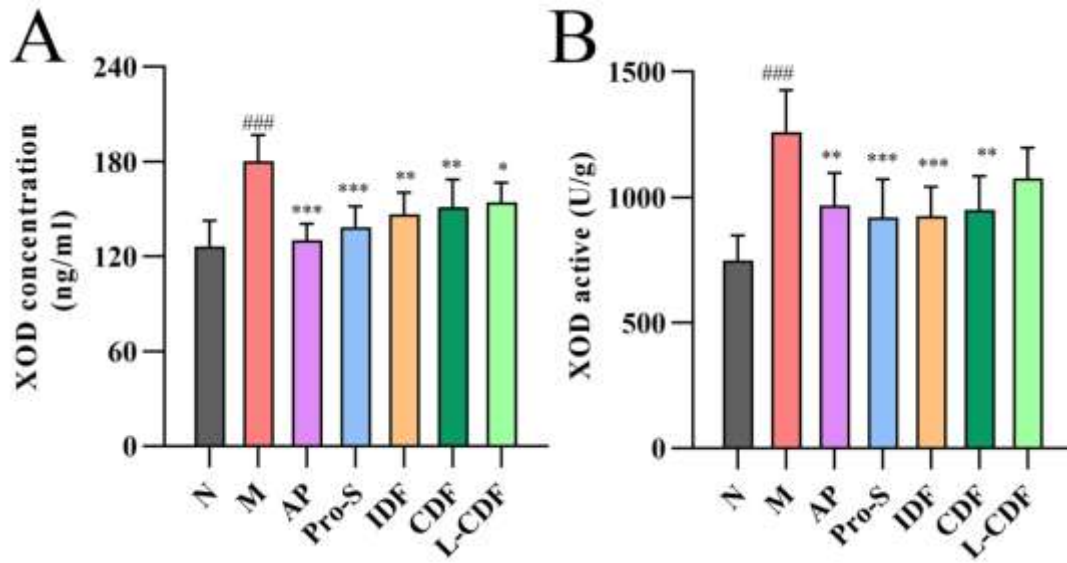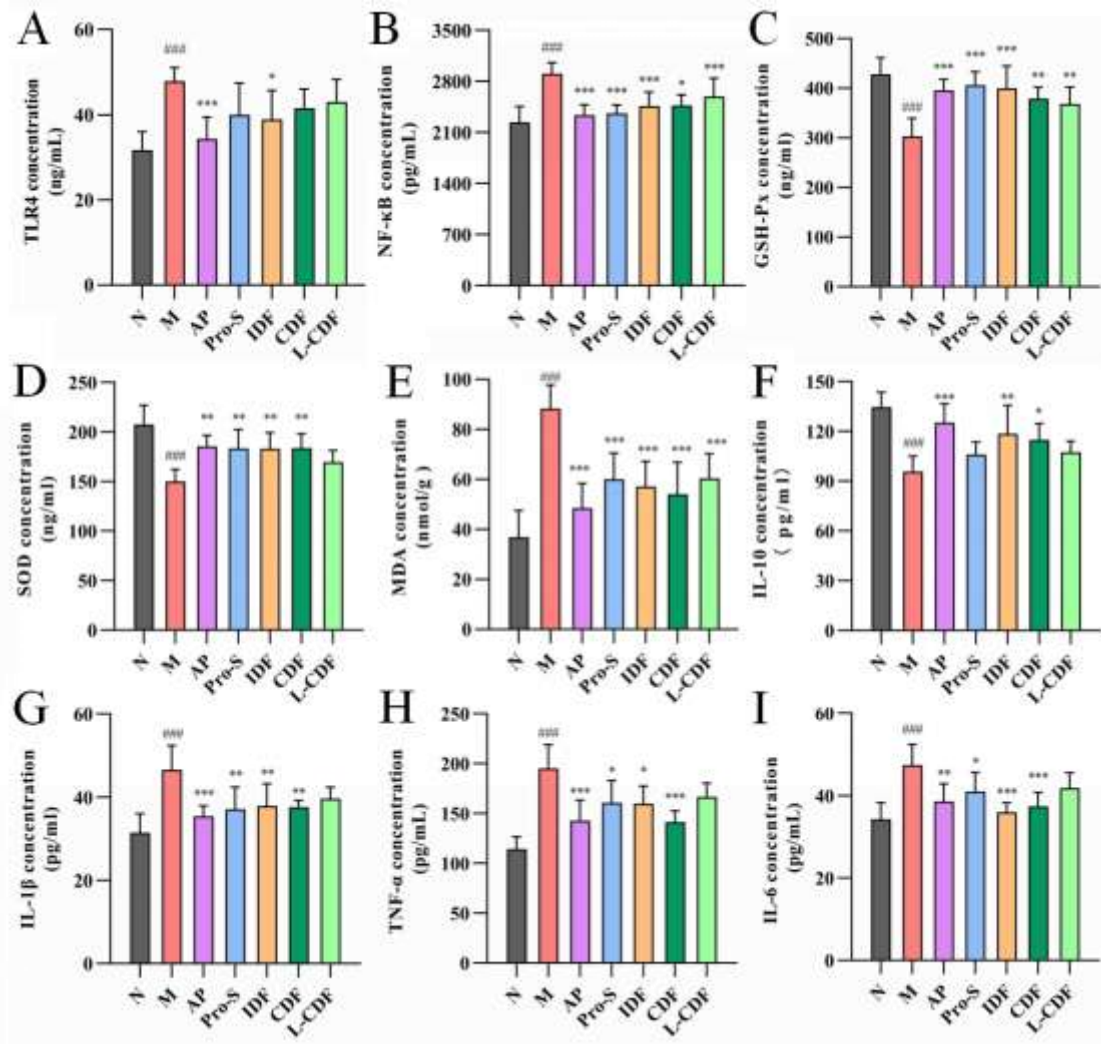
Fig. 2 The effect of DF on XOD content and active in the liver. A XOD concentration, and B XOD active in liver. $*P < 0.05; **P < 0.01; ***P < 0.001$ represent significance between each group compared with M group. $\#P < 0.05; \#\#P < 0.01; \#\#\#P < 0.001$ represent significance between M group compared with N group.

Fig. 3 DF slows down oxidative stress and inflammatory responses. A TLR4 concentration. B NF-κB concentration.C SOD concentration.D GSH-Px concentration. E MDA concentration.F IL-10 concentration.G IL-1β concentration.H TNF-α concentration.I IL-6 concentration. $*P < 0.05$;$**P < 0.01$; $***P < 0.001$ represent significance between each group compared with M group. $\#P < 0.05$; $\#\#P < 0.01$; $\#\#\#P < 0.001$ represent significance between M group compared with N group.
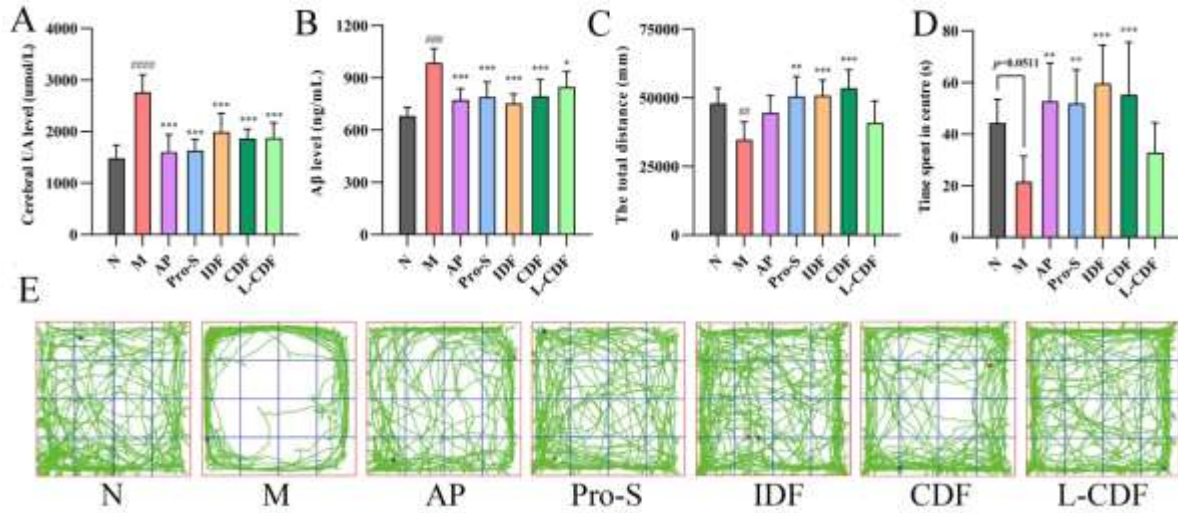
Fig. 4 DF reduces Aβ deposition and alleviates neuroanxiety. A Cerebral UA level. B Aβ level. C The tltal distance,and D Time spent in centre. E Representative exploration traces of OFT. $*P < 0.05$;$**P < 0.01$; $***P < 0.001$ represent significance between each group compared with M group. $\#P < 0.05$; $\#\#P < 0.01$; $\#\#\#P < 0.001$ represent significance between M group compared with N group.
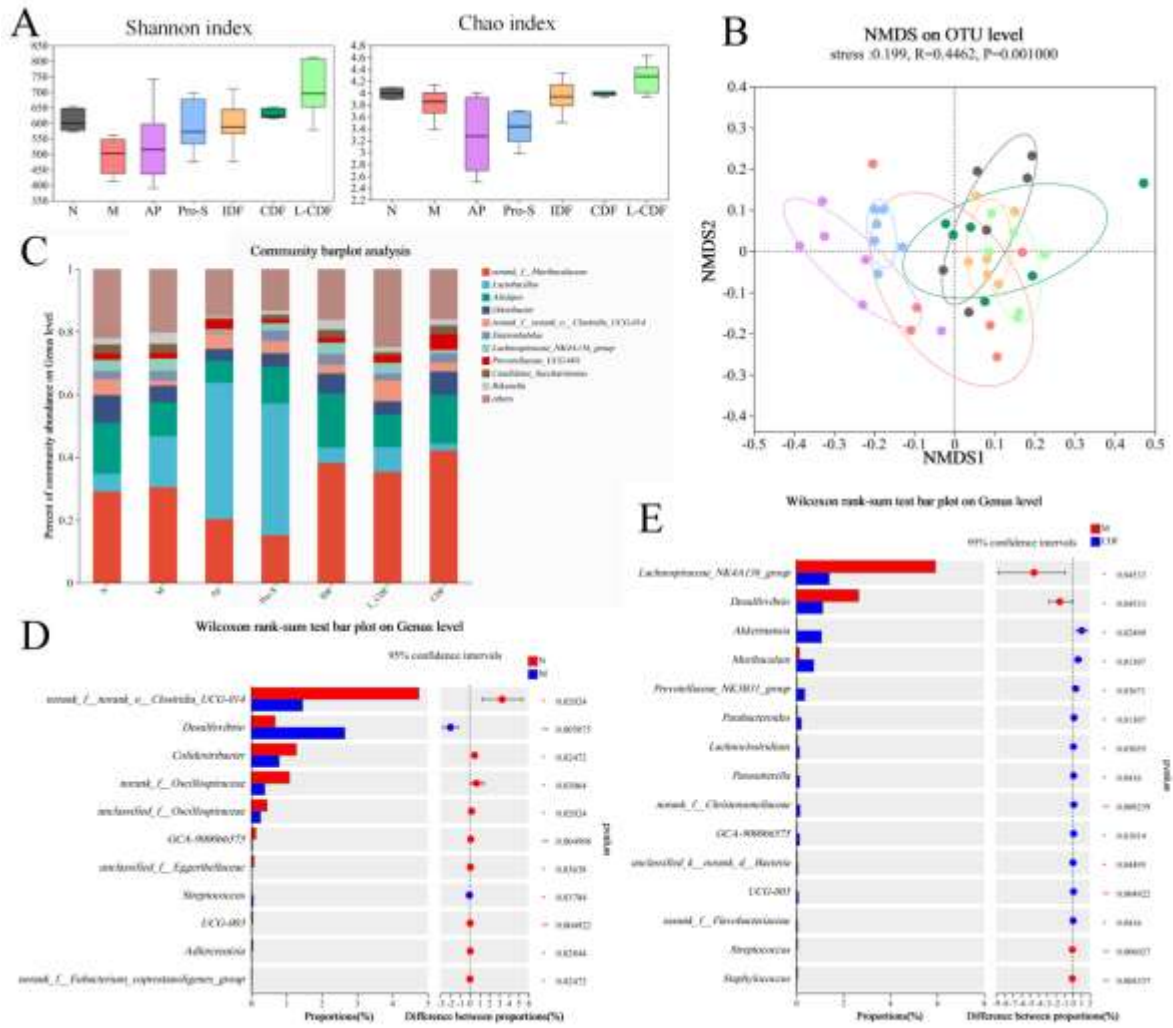
Fig. 5 CDF changed the structure of gut microbiota in HUA mice. A Chao index and Shannon index in each group. B NMDS analysis of gut microbiota on OTU level in each group. C Relative abundance changes of gut microbiota on genus level. D The comparison of bacterial microbiota between M and N at genus level. E The comparison of bacterial microbiota between M and CDF at genus level.
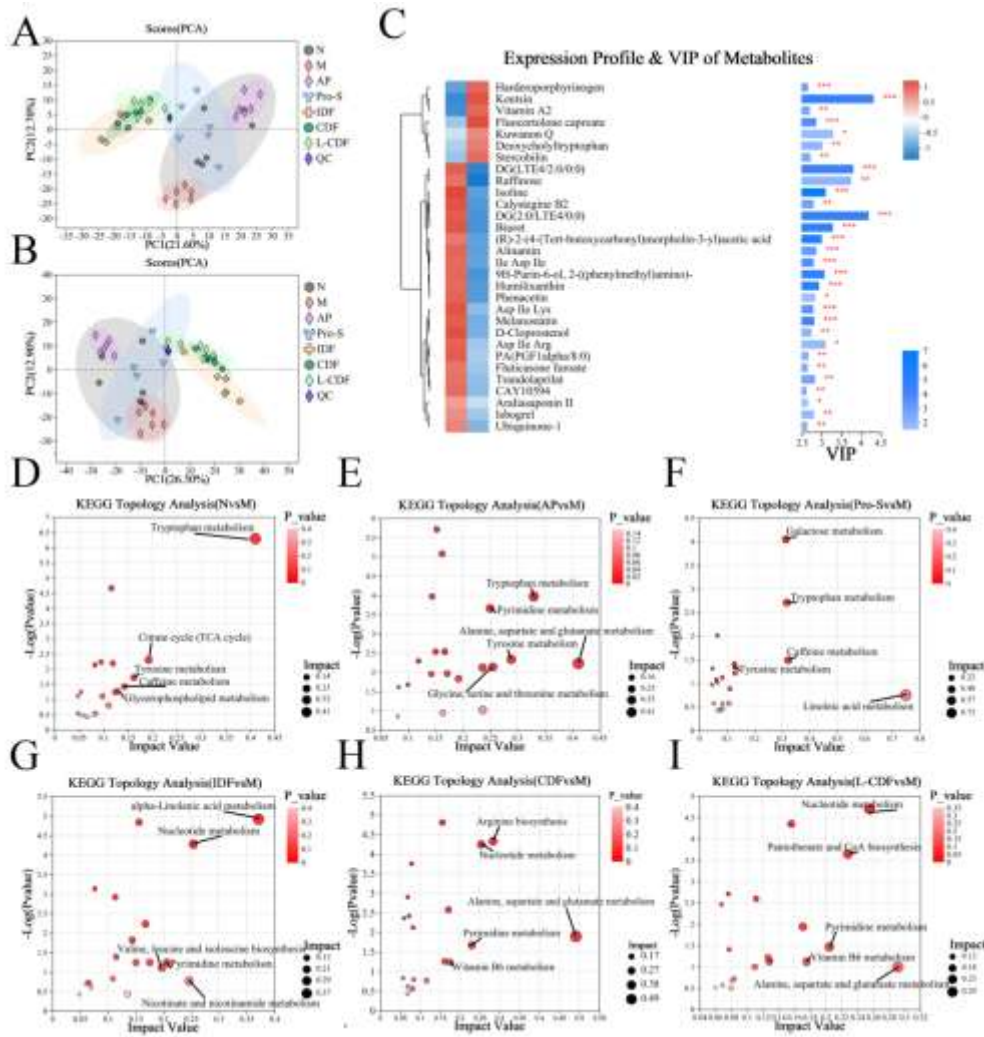
Fig. 6 Effect of CDF on metabolism of HUA mice. A Scores plot of PCA analysis of all samples of positiveion mode. B Scores plot of PCA analysis of all samples of negativeion mode. C Expression profile, VIP score, and P-value of the top 30 differential serum metabolites in M compared with N. Detection of the metabolic pathway topology analysis. D N Group vs M group. E AP group vs M group. F AP group vs M group. G IDF group vs M group. H CDF group vs M group. I L-CDF group vs M group. Each bubble represents a metabolic pathway.

Fig. 7 Spearman correlation analysis of the gut microbiota and metabolomics. Note: The red oval indicates a positive correlation and the blue oval indicates a negative correlation between the gut microbiota and metabolomics.
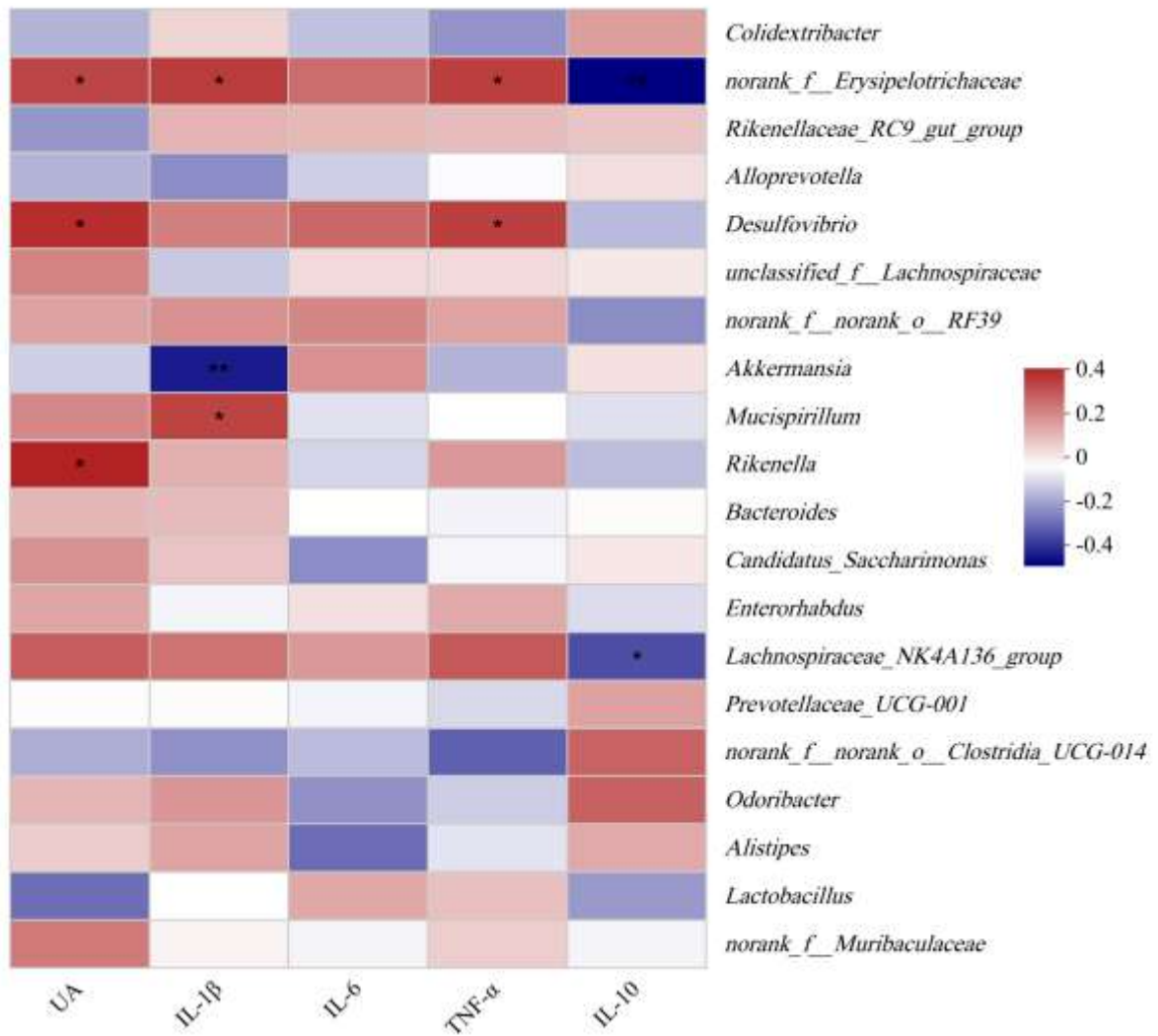
Fig. 8 Correlation analysis of gut microbiota and inflammatory factors. Note: The red oval indicates a positive correlation and the blue oval indicates a negative correlation between the gut microbiota and inflammatory factors.